REGULAR ARTICLE

blood advances

Mesenchymal stromal cells ameliorate chronic GVHD by boosting thymic regeneration in a CCR9-dependent manner in mice

Xin Zhang,[1,2,*] Jiabao He,[1,3,*] Ke Zhao,[1,3,*] Shiqi Liu,[1,3,*] Li Xuan,[1,3] Shan Chen,[1,3] Rongtao Xue,[1,3] Ren Lin,[1,3] Jun Xu,[1,3] Yan Zhang,[1,3] Andy Peng Xiang,[4] Hua Jin,[1,3] and Qifa Liu[1,3]

[1]Department of Hematology, Nanfang Hospital, Southern Medical University, Guangzhou, China; [2]Department of Hematology, The First Affiliated Hospital of Soochow University, Suzhou, China; [3]Clinical Medical Research Center of Hematology Diseases of Guangdong Province, Guangzhou, China; and [4]Center for Stem Cell Biology and Tissue Engineering, Key Laboratory for Stem Cells and Tissue Engineering, Sun Yat-Sen University, Guangzhou, China

Key Points

- MSCs decrease the incidence and severity of experimental cGVHD.
- MSCs can home to the thymus via the CCL25-CCR9 axis and repair the damaged thymus caused by aGVHD.

Chronic graft-versus-host disease (cGVHD) is a major cause of morbidity and mortality after allogeneic hematopoietic stem cell transplantation. Mature donor T cells within the graft contribute to severe damage of thymic epithelial cells (TECs), which are known as key mediators in the continuum of acute GVHD (aGVHD) and cGVHD pathology. Mesenchymal stromal cells (MSCs) are reportedly effective in the prevention and treatment of cGVHD. In our previous pilot clinical trial in patients with refractory aGVHD, the incidence and severity of cGVHD were decreased, along with an increase in levels of blood signal joint T-cell receptor excision DNA circles after MSCs treatment, which indicated an improvement in thymus function of patients with GVHD, but the mechanisms leading to these effects remain unknown. Here, we show in a murine GVHD model that MSCs promoted the quantity and maturity of TECs as well as elevated the proportion of Aire-positive medullary TECs, improving both $CD4^+CD8^+$ double-positive thymocytes and thymic regulatory T cells, balancing the CD4:CD8 ratio in the blood. In addition, CCL25-CCR9 signaling axis was found to play an important role in guiding MSC homing to the thymus. These studies reveal mechanisms through which MSCs ameliorate cGVHD by boosting thymic regeneration and offer innovative strategies for improving thymus function in patients with GVHD.

Introduction

Chronic graft-versus-host disease (cGVHD) remains a major cause of morbidity and mortality following allogeneic hematopoietic stem cell transplantation (allo-HSCT).[1-3] cGVHD can occur without previous acute GVHD (aGVHD); however, most cGVHDs occur after the evolvement from aGVHD.[4] The pathogenesis and high incidence of cGVHD in patients with aGVHD remains poorly understood. Emerging evidence from murine studies suggests that the pathogenesis may be related to thymus damage caused by aGVHD.[5-11] The thymus is 1 of the important central immune organs and plays a critical role in the development of T cells. T-cell reconstitution after allo-HSCT is mainly accomplished by thymus-independent and thymus-dependent mechanisms. The thymus-independent pathway occurs early after transplantation and depends on the peripheral expansion of mature donor T cells; although

Submitted 30 December 2022; accepted 18 June 2023; prepublished online on *Blood Advances* First Edition 26 June 2023; final version published online 15 September 2023. https://doi.org/10.1182/bloodadvances.2022009646.

*X.Z., J.H., K.Z., and S.L. contributed equally to this study.

All relevant data supporting the findings of this study are available within the paper, its supplementary information, and on request from the corresponding authors, Qifa Liu (liuqifa628@163.com), Hua Jin (echohua1124@163.com), and Andy Peng Xiang (xiangp@mail.sysu.edu.cn).

The full-text version of this article contains a data supplement.

© 2023 by The American Society of Hematology. Licensed under Creative Commons Attribution-NonCommercial-NoDerivatives 4.0 International (CC BY-NC-ND 4.0), permitting only noncommercial, nonderivative use with attribution. All other rights reserved.

Downloaded from http://ashpublications.net/bloodadvances/article-pdf/7/18/5359/2079881/blooda_adv-2022-009646-main.pdf by guest on 12 June 2024

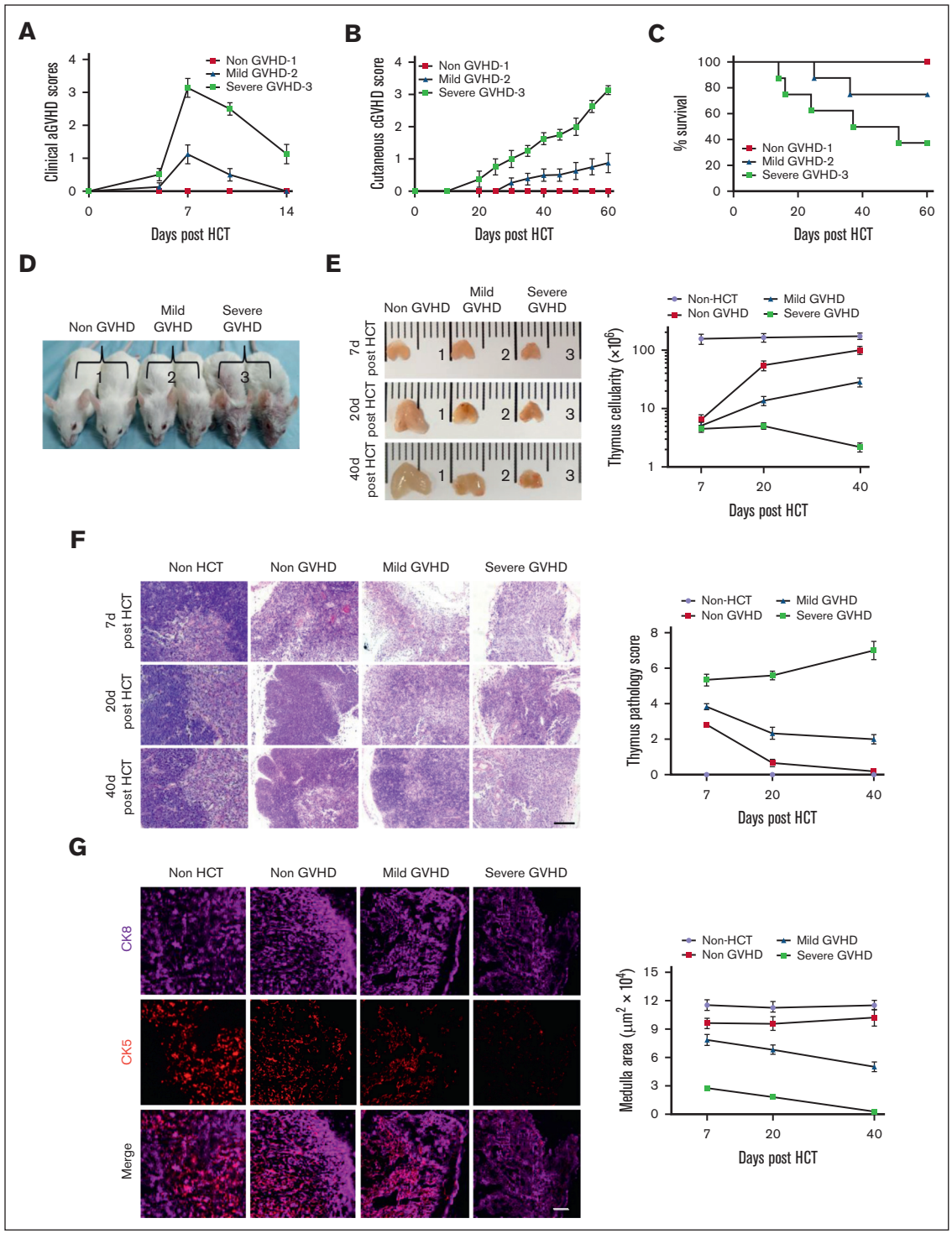

Figure 1. The degree of thymus damage was associated with severity of cGVHD. TCD-BM alone (~2.5 × 10^6 cells, non-GVHD) or TCD-BM (2.5 × 10^6 cells) plus 1 × 10^6 cells splenocytes (severe-GVHD) or 0.25 × 10^6 splenocytes (mild-GVHD) from C57BL/6 mice were transplanted into BALB/c mice. Mice were monitored for aGVHD clinical symptoms, cutaneous cGVHD, and survival. Thymus structure were assessed 7, 20, and 40 days after HCT, with H&E staining. (A-C) aGVHD symptom scores, cutaneous cGVHD score, and percentage of survival. Each group contained between 12 and 16 recipients combined from 3 replicate experiments. (D) Picture taken on day 40 after HCT (1, non-GVHD; 2, Mild-GVHD; and 3, severe-GVHD). (E) The appearance of the thymus (n = 3) and thymus cellularity of each group results are shown as mean ± standard error (SE) (n = 6). (F) Representative photomicrographs of H&E-stained thymus tissue section and thymus pathology score, results are shown as mean ± SE (n = 6); scale bar, 50 μm. (G) Forty days after transplantation, thymuses were harvested and identified via immunofluorescent staining of CK8 (purple, highly expressed in cortex and lowly expressed in medulla) and CK5 (red, expressed in medulla), and medulla area was measured and shown as mean ± SE (n = 6); scale bar, 50 μm.

Downloaded from http://ashpublications.net/bloodadvances/article-pdf/7/18/5359/2079881/blooda_adv-2022-009646-main.pdf by guest on 12 June 2024

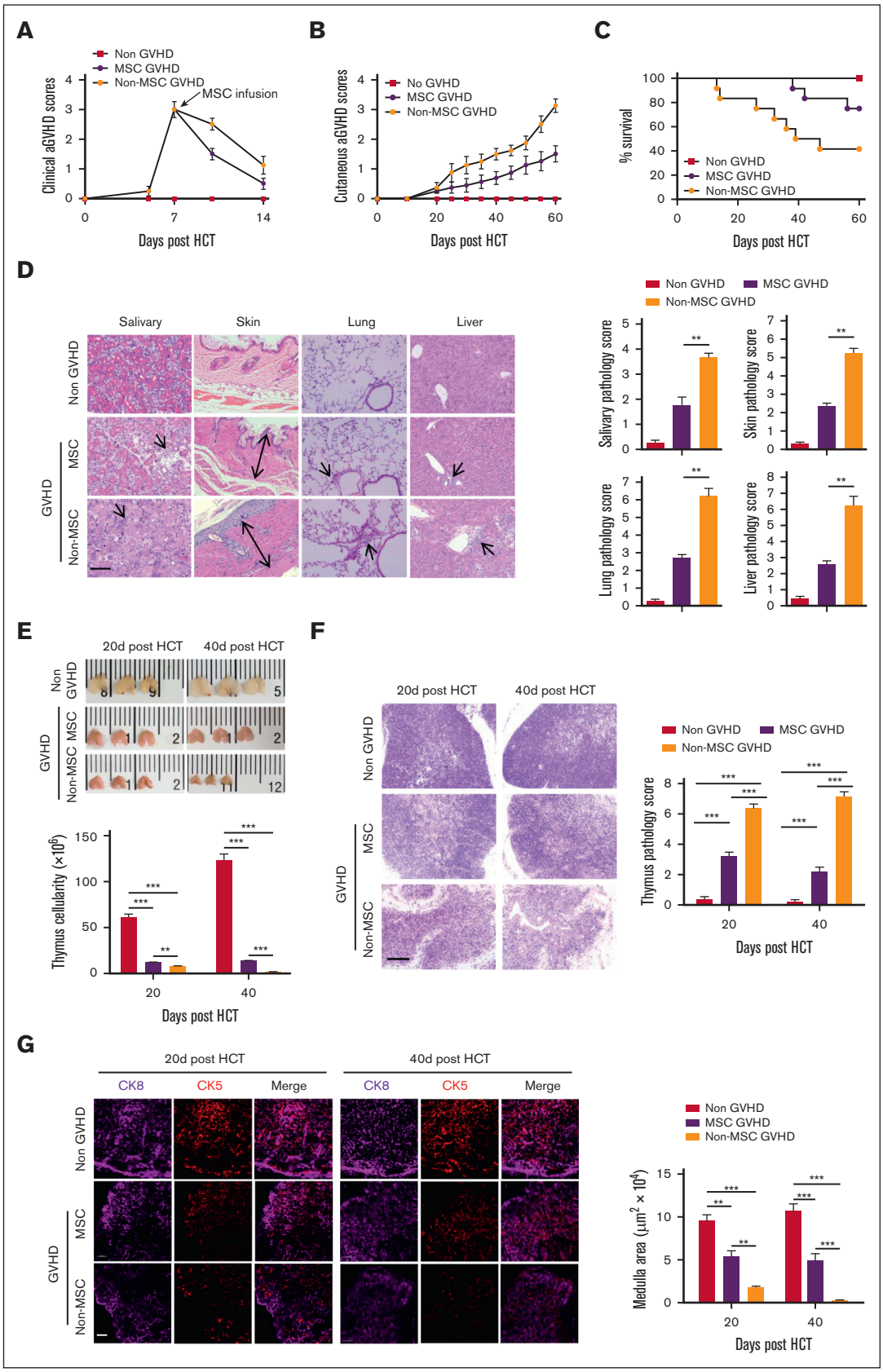

Figure 2.

Downloaded from http://ashpublications.net/bloodadvances/article-pdf/7/18/5359/2079881/blooda_adv-2022-009646-main.pdf by guest on 12 June 2024

such an allo-immune process can cure the underlying disease, it may also cause GVHD. The thymus-dependent pathway rebuilds naïve T cells with self-tolerance and perfect function from donor lymphoid stem cells,[7] which depends on thymus stromal cells that provide an appropriate thymic microenvironment, particularly thymic epithelial cells (TECs) that are responsible for positive and negative selection.[12,13] Mature donor T cells within the graft preferentially damage recipient medullary TECs (mTECs) and impair negative selection, resulting in production of autoreactive T cells that perpetuate damage to the thymus and augment the development of cGVHD.[8]

Mesenchymal stromal cells (MSCs) are multipotent progenitor cells that reside in many adult tissues.[14] Based on their multipotent and immunomodulatory properties, MSCs have been successfully used in tissue repair and treatment of autoimmune diseases, including GVHD.[15-17] Some studies have demonstrated that MSCs are effective in the prevention and treatment of cGVHD.[18-20] However, the therapeutic mechanisms by which MSCs ameliorate cGVHD remains poorly understood. In our pilot clinical trial of patients with refractory aGVHD receiving MSCs treatment, we found that the incidence and severity of cGVHD decreased, along with increased signal joint T-cell receptor excision DNA circles in the blood, compared with those in control patients.[21] These results suggest that MSCs might exert immunomodulatory effects through the thymus. A few studies performed by our group and other groups have implicated MSCs could home to the damaged thymus and improve thymus function in murine models,[22-24] but the specific mechanism of homing and repairing the thymus awaits clarification.

For MSCs to home to the target organ, the right combination and interaction of chemokine and the corresponding chemokine receptor are required.[25,26] Chemokine C-C motif ligand 25 (CCL25), also known as thymus-expressed chemokine, is first found in the thymus. Thymic dendritic cells in the medullary region, TECs, and intestinal epithelial cells constitute the predominant source of CCL25.[27] Chemokine receptor 9 (CCR9), expressed on T-lineage precursors as well as on MSCs is the only specific receptor for CCL25.[28,29] By analyzing the migration properties of MSCs, researchers discovered that CCL25 holds great promise in specifically targeted MSCs attraction, being the only chemokine showing highly specific MSCs migration toward CCL25 gradients in various migration assays.[30-32] This motivated researchers to apply CCL25 in specific (ie, injured) tissues to recruit MSCs and, thus, foster in situ regeneration.[31,33] Theoretically, as an organ that highly expresses CCL25, the thymus has the natural advantage of attracting MSCs. Therefore, we proposed that MSCs home to the damaged thymus of mice with GVHD via the CCL25-CCR9 axis and that MSCs reduce the incidence and severity of cGVHD by boosting thymic regeneration. To further verify this hypothesis, we investigated the effects of MSCs in the thymus of patients with GVHD using a murine GVHD model that undergoes both aGVHD and cGVHD stages.

Methods

Mice

C57BL/6 (H-2^b) and BALB/c (H-2^d) mice were obtained from the Animal Experiment Center of Southern Medical University, and the enhanced green fluorescent protein (EGFP) transgenic C57BL/6J mice were purchased from the Model Animal Research Center of Nanjing University and The Jackson Laboratory. Male, 8 to 12-week-old C57BL/6 and BALB/c mice were used for GVHD modeling; 2 to 3-week-old EGFP-transgenic C57BL/6J mice were used for the isolation of murine MSCs. Mice were maintained in a pathogen-free room at the Animal Institute of Southern Medical University. All animal protocols were approved by the Southern Medical University institutional animal care and use committee.

Isolation, culture, and identification of murine MSCs

MSCs were isolated from the compact bone of wild-type or EGFP-transgenic C57BL/6J mice based on their different purposes.[34] Briefly, the femurs and tibias were dissected and the bone marrow (BM) cells thoroughly depleted by flushing with α–minimum essential medium (MEM; Gibco, Australia). Subsequently, the bones were chopped into chips and digested with collagenase II (1 mg/mL, Gibco) for 1 to 2 hours. After digestion, bone chips were washed 3 times with 5 mL of α-MEM and seeded into a culture flask in the presence of 6 mL α-MEM supplemented with 10% fetal bovine serum (Gibco). On the third culture day, nonadherent cells were removed and replaced with fresh medium. Adherent cells were further cultured, with a change of medium every 3 days. When the monolayers reached 80% to 90% confluence, the cells were detached and passaged. Cells were harvested after 8 passages and identified based on antigen expression using flow cytometry as well as based on adipogenic and osteogenic differentiation capacity (supplemental Figure 5), before being administered to GVHD mice.

Induction and assessment of murine GVHD

BALB/c mice were irradiated at a dose of 850 cGy, 8 hours before hematopoietic cell transplantation (HCT). Recipients were injected with 2.5×10^6 T-cell–depleted donor BM cells (TCD-BM) alone or 2.5×10^6 TCD-BM together with 0.25×10^6 or 1×10^6 splenocytes from C57BL/6 donors. T-cell depletion was achieved using biotin-conjugated anti-CD3, anti-CD4, and anti-CD8 and streptavidin–conjugated magnetic beads, followed by passaging through an auto-MACS cell sorter (Miltenyi Biotec). The purity of depletion was >99%.

Figure 2. MSCs ameliorate cGVHD. Mice with severe GVHD were treated with MSCs (MSC-GVHD) or normal saline (non–MSC-GVHD) on day 7 after HCT (aGVHD symptoms peak). Non-GVHD mice served as control. Mice were monitored for aGVHD clinical symptoms, cutaneous cGVHD, survival, and histopathology of cGVHD target tissues. Thymus size and structure were assessed on day 20 and day 40 after HCT with H&E and immunofluorescent staining. (A-C) aGVHD symptom scores, cutaneous cGVHD symptom score, and survival curve. Each group contained between 12 and 16 recipients combined from 3 replicate experiments. (D) Representative photomicrographs of the salivary gland, skin, lung, and liver. Histopathology scores are shown as mean ± SE (n = 4-6); scale bar, 50 μm. Arrows indicate the following: infiltration and loss of ductal structure in the salivary gland; hyperplasia in the epidermis, expansion of the dermis, and loss of subcutaneous fat; perivascular and peribronchiolar infiltration; infiltration in the liver, involved tracts, and liver cell necrosis. (E) Representative photographs of the thymus, and thymus cellularity in each group, results are shown as mean ± SE (n = 6). (F) Representative photomicrographs of H&E-stained thymus tissue section (scale bar, 50 μm) and thymus pathology score, results are shown as mean ± SE (n = 6). (G) Medulla area in the thymus was measured by immunofluorescent staining for CK8 and CK5, results are shown as mean ± SE (n = 4-6); scale bar, 50 μm. $^{**}P < .01$; $^{***}P < .001$. ns, not significant.

Downloaded from http://ashpublications.net/bloodadvances/article-pdf/7/18/5359/2079881/blooda_adv-2022-009646-main.pdf by guest on 12 June 2024

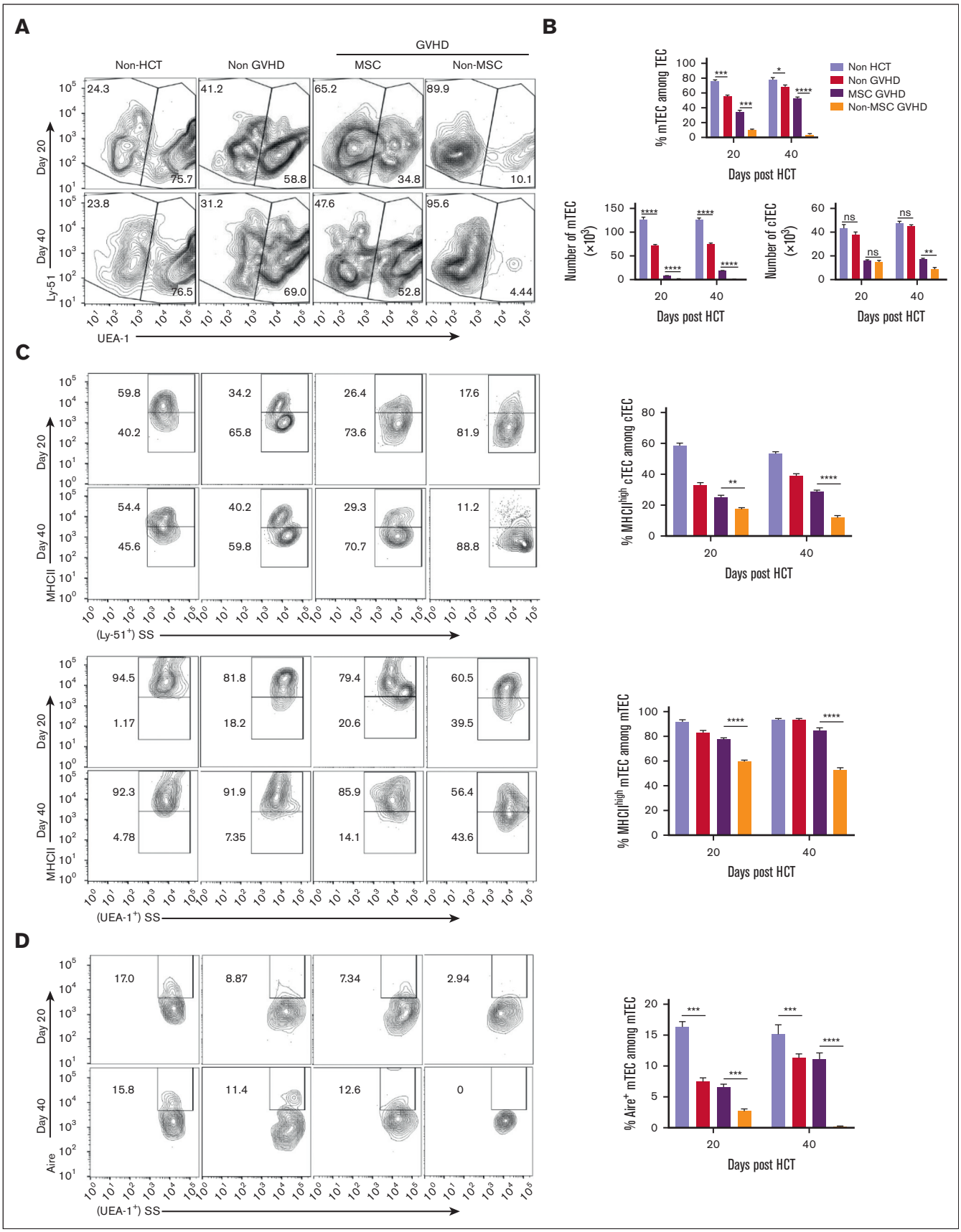

Figure 3.

Downloaded from http://ashpublications.net/bloodadvances/article-pdf/7/18/5359/2079881/blooda_adv-2022-009646-main.pdf by guest on 12 June 2024

The assessment of GVHD included clinical symptoms and pathology of target organs, which were performed per previous publications, with some modifications.[10,35,36] The aGVHD clinical symptoms scoring system included weight loss, posture, activity, and diarrhea. A scale from 0 to 2 was used for each category of the symptom (supplemental Table 1), and composite symptom scores were determined by taking the sum of the individual scores for each mouse. Clinical cGVHD was evaluated and scored based on the development of alopecia and ulcers on hair-bearing skin. Ulcers or scaling in non–hair-bearing skin (ears, tails, and paws) were also examined for scoring (supplemental Table 2).

The jejunum and colon were evaluated as aGVHD target organs, whereas the salivary glands, skin, lung, and liver were assessed as cGVHD target organs. Hematoxylin and eosin (H&E) staining on formalin-fixed, paraffin-embedded tissue slides were used for evaluation. Slides were examined at magnification ×200, and tissue damage was assessed by an experienced pathologist blinded to the identity of the groups. Jejunum GVHD was scored based on intestinal damage, including villous blunting, crypt regeneration, crypt epithelial cell apoptosis, crypt loss, luminal sloughing of cellular debris, lamina propria inflammatory cell infiltrate, and mucosal ulceration, and the maximum score was 14. Colon GVHD histopathology was evaluated for increased mononuclear cell infiltration and morphological aberrations (eg, hyperplasia and crypt loss), with a maximum score of 10. Salivary GVHD was evaluated based on mononuclear cell infiltration and structural disruption, with a maximum score of 8. Skin GVHD was scored based on the damage in the epidermis and dermis, judged based on the hyperplasia of epidermis, enlargement, fibrosis of dermis, and loss of subcutaneous fat, with a maximum score of 9. Lung tissue was evaluated on a scoring system based on perivascular and peribronchiolar infiltration and inflammation; the maximum score was 9. The liver was scored based on the number of involved tracts and the severity of lymphocytic infiltration and liver cell necrosis, with a maximum score of 9.

Thymus structure assessment

Thymus structure was assessed using H&E and immunofluorescent staining. The pathology of the thymus was evaluated based on a decrease in cortical cellularity, loss of cortex/medulla demarcation, and the reduction of Hassall corpuscles by H&E staining, with a maximum score of 9. For immunofluorescent staining, the thymus was embedded in optimum cutting temperature compound and 6-μm thick cryosections were used. The cryosections were stained with rat anti-mouse cytokeratin 8 (CK8, Developmental Studies Hybridoma Bank) for both cortical (CK8 high expressed) and medullary (CK8 low expressed) thymus epithelial cells, and rabbit anti-mouse cytokeratin 5 (CK5, Abcam) for medullary epithelial cells, followed by Alexa Fluor 555–labeled donkey anti–rabbit immunoglobulin G and Alexa Fluor 647–labeled donkey anti–rat immunoglobulin G (Jackson Immuno Research). The medulla area in the thymus was measured based on CK5 expression along with lowly expressed CK8 using a Zeiss fluorescence microscope.

Flow cytometry analysis

The antibodies and reagents used for flow cytometry analysis are listed: anti-mouse antibodies, CD11b (clone M1/70), CD29 (HMb1-1), CD31 (390), CD34 (RAM34), CD44 (IM7), CD45 (30-F11), CD105 (MJ7/18), CD106 (429), CD140a (APA5), Sca-1 (Ly-6A/E, D7), CD3(17A2), CD4 (GK1.5), CD8a (53-6.7), CD25 (PC61.5), FoxP3 (FJK-16s), T-cell receptor Vβ 5.1/5.2 (MR9-4), CD326 (EpCAM, G8.8), Ly51(BP-1, 6C3), Aire (5H12), CCR9 (CD199, CW-1.2), and allophycocyanin-labeled streptavidin (17-4317-82), which were obtained from eBioscience. Biotinylated *Ulex europaeus* agglutinin-1 (UEA-1, #B1065) was purchased from Vector Laboratories. The Foxp3 permeabilization/fixation kit (eBioscience) was used for cell fixation/permeabilization during intracellular staining. Aqua fluorescent reactive dye for viability analysis (L34957) was obtained from Invitrogen. All staining was performed per the manufacturers' instructions. Labeled cells were analyzed on a BD FACS Canto II (BD Biosciences, Franklin Lakes, NJ) and data analyzed using the FlowJo software. The gating strategies are shown in the supplemental Figure 6.

Overexpression and knockdown of CCR9 in murine MSCs

Lentivirus to overexpress CCR9 and lentivirus that encoded CCR9-specific short hairpin RNA were designed and constructed by GeneChem (Shanghai, China). For lentiviral transduction, CCR9 wild-type MSCs ($MSCs^{CCR9WT}$) isolated from EGFP-transgenic mice at passage 4 were dissociated into single-cell suspensions using 0.125% TrypLE Select (Invitrogen) and then replated with the 2 lentiviral particles. The cells were selected in 2 μg/mL puromycin (Invivogen, Germany) starting at 24 hours after infection. Stably transfected MSCs (referred to as $MSCs^{CCR9+}$ and $MSCs^{CCR9-}$) were cultured continuously after selection. Overexpression and knockdown of CCR9 was confirmed via quantitative reverse transcription polymerase chain reaction and flow cytometry.

MSCs home to the thymus

To explore the role of CCR9 in MSC homing to the thymus, EGFP-expressing $MSCs^{CCR9WT}$, $MSCs^{CCR9+}$, and $MSCs^{CCR9-}$, respectively, were administrated to GVHD mice IV on day 7 after HCT. Thymus glands were collected from $MSCs^{CCR9WT}$ GVHD, $MSCs^{CCR9+}$ GVHD, and $MSCs^{CCR9-}$ GVHD mice on days 1, 7, and 14 after MSCs infusion. Cryosections were prepared and counterstained with 1.0 mg/mL 4′,6-diamidino-2-phenylindole in phosphate-buffered saline for 20 minutes at room temperature in the dark. The distribution of $EGFP^+$ cells was analyzed with Zeiss fluorescence microscope.

Statistical analysis

Data analysis was performed and displayed using GraphPad Prism, version 6.0. Data are displayed as mean ± standard error. Clinical GVHD scoring, tissue damage scoring, and survival in different groups were compared using the multiple *t* test or log-rank test. Comparison of 2 means was with an unpaired 2-tailed Student *t*

Figure 3. MSCs induce thymic regeneration by repairing TECs. The proportion, number, and major histocompatibility complex class II (MHC II) levels of TECs, and Aire expression on mTECs were assessed in MSC-GVHD, non–MSC-GVHD, and non-GVHD recipients on day 20 and day 40 after HCT via flow cytometry. (A) Representative flow patterns of gated TECs shown as UEA-I (mTEC marker) vs Ly-51 (cortical TEC [cTEC] marker). (B) The proportion and number of mTECs and number of cTECs on day 20 and days 40 after HCT, data shown as the mean ± SE (n = 4-6). (C) Gated mTECs and cTECs shown as MHC II vs side scatter area (SSC-A). The percentage data of $MHC\ II^+$ are shown as mean ± SE (n = 4-6). (D) Gated mTECs shown as Aire vs SSC-A. The percentage data of Aire-positive mTECs are shown as mean ± SE (n = 4-6). $^{**}P < .01$; $^{***}P < .001$; $^{****}P < .0001$.

Downloaded from http://ashpublications.net/bloodadvances/article-pdf/7/18/5359/2079881/blooda_adv-2022-009646-main.pdf by guest on 12 June 2024

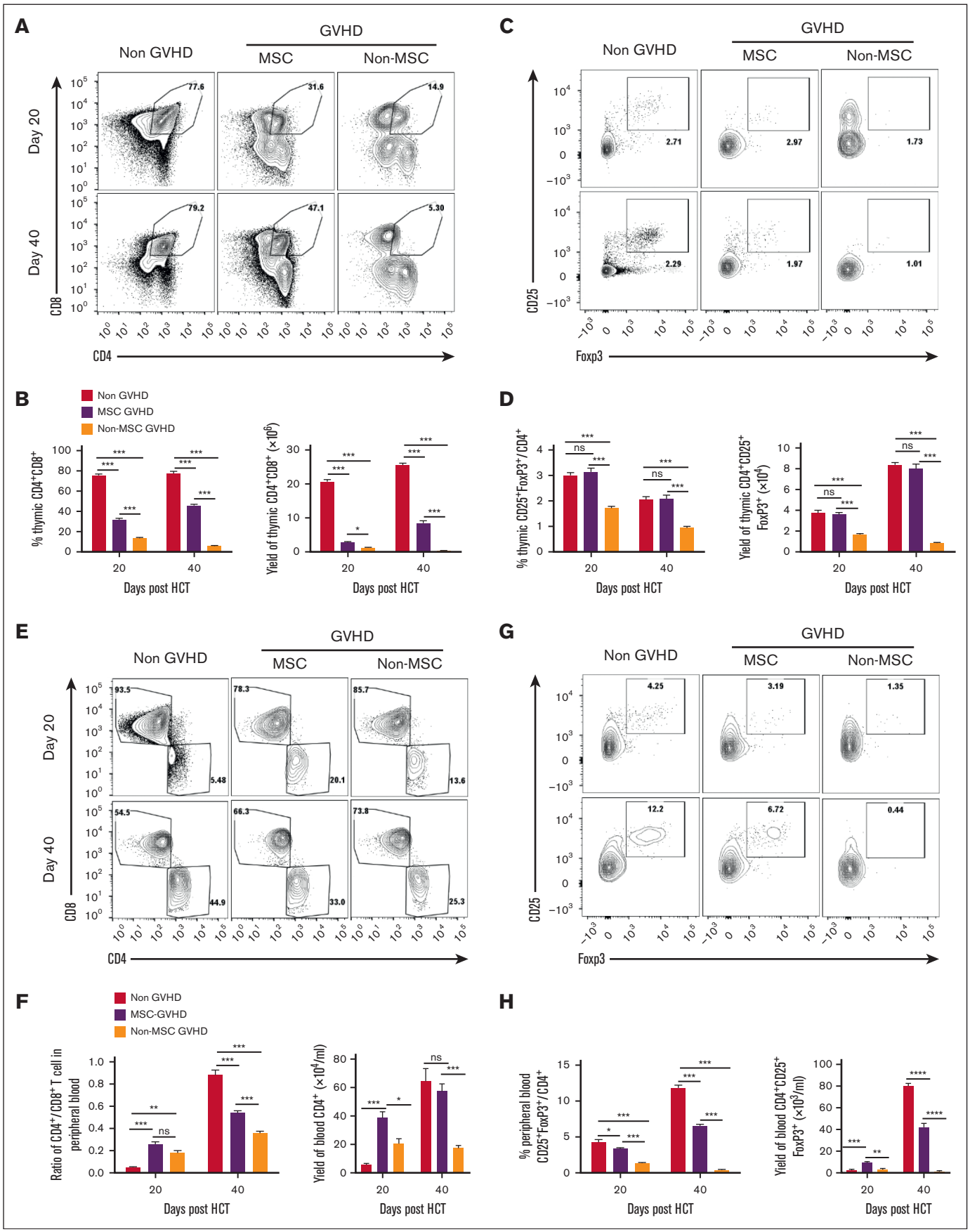

Figure 4.

Downloaded from http://ashpublications.net/bloodadvances/article-pdf/7/18/5359/2079881/blooda_adv-2022-009646-main.pdf by guest on 12 June 2024

test; comparison of multiple means was with one-way analysis of variance.

Results

Thymus damage induced by aGVHD positively correlates with cGVHD

To confirm the role of the thymus in cGVHD pathogenesis, BALB/c mice were injected with TCD-BM alone or TCD-BM plus 2 different dosages (1×10^6 or 0.25×10^6) of splenocytes from C57BL/6 donors. The results showed that the mice that received 1×10^6 splenocytes developed moderate aGVHD ~5 to 9 days after HCT, followed by severe cGVHD ~35 to 45 days after HCT (severe-GVHD). Moreover, ~40% of the mice survived >60 days. Recipients who received 0.25×10^6 splenocytes developed mild aGVHD and mild cGVHD (mild-GVHD), and ~80% of them survived >60 days. Recipients with TCD-BM alone showed no manifestations of GVHD (non-GVHD) (Figure 1A-D; supplemental Figure 1).

Thymus structure and cellularity in severe-GVHD, mild-GVHD, and non-GVHD mice were assessed 7, 20, and 40 days after HCT. It was observed that the thymus of severe-GVHD, mild-GVHD, and non-GVHD mice all displayed shrinking on day 7 after HCT, and the thymus cellularity among the 3 groups showed no significant difference. Compared with the non-HCT group, thymus cellularity gradually recovered in the non-GVHD mice and partially recovered in the mild-GVHD mice by day 20 and 40 after HCT; however, no recovery was observed in severe-GVHD mice (Figure 1E). H&E staining of the tissue revealed distinct corticomedullary demarcation in non-GVHD mice on day 7 after HCT, whereas the corticomedullary demarcation was unclear or lost in the thymus of both the mild-GVHD and severe-GVHD mice. The thymus structure was substantially or partially recovered in both the non-GVHD and mild-GVHD mice 20 and 40 days after HCT but got worse in severe-GVHD mice (Figure 1F). Immunofluorescent staining showed well-formed $CK8^+$ cortex and $CK5^+$ medulla in the non-GVHD mice 7, 20, and 40 days after HCT. Furthermore, the $CK5^+$ medulla area was slightly reduced in mild-GVHD mice at similar time points compared with that in non-GVHD mice, whereas it was significantly reduced in the severe-GVHD mice, which was almost undetectable 40 days after HCT (supplemental Figure 2; Figure 1G).

These results suggest that thymus damage caused by preconditioning (radiotherapy) alone is partially reversible, and the severity of cGVHD correlates with the degree of thymus damage.

MSCs administrated at aGVHD stage ameliorate cGVHD

To investigate whether MSCs administrated at the aGVHD phase could ameliorate cGVHD, severe-GVHD mice were IV treated with MSCs from EGFP-transgenic C57BL/6J mice at a dose of 1×10^6 cells per mouse (MSC-GVHD) or normal saline (non–MSC-GVHD) 7 days after HCT (aGVHD symptoms peak); the non-GVHD mice served as controls. More rapid improvement of aGVHD symptoms was observed ~3 days after MSCs infusion compared with that in non–MSC-GVHD mice (Figure 2A). The cutaneous cGVHD score in the MSC-GVHD mice was lower than that in the non–MSC-GVHD mice 40 days after HCT (Figure 2B). Moreover, the MSC-GVHD mice gained enhanced survival, with ~75% surviving for >60 days after HCT compared with ~40% of the non–MSC-GVHD mice (Figure 2C). Histopathological analysis of cGVHD target organs showed less injuries in the MSC-GVHD mice than in the non–MSC-GVHD mice 60 days after HCT (Figure 2D).

Thymus structure and cellularity were assessed on days 20 and 40 after HCT. The results showed that MSC-GVHD mice displayed less thymic atrophy and enhanced thymus cellularity than the non–MSC-GVHD mice 20 and 40 days after HCT (Figure 2E). The thymus of MSC-GVHD mice showed less tissue damage with increased cell density in the cortex, recovered corticomedullary demarcation (Figure 2F), and ameliorated medulla area compared with non–MSC-GVHD mice at both time points (Figure 2G).

These results indicated that MSCs administrated at the aGVHD stage effectively decreased the incidence and severity of cGVHD, which was related to repaired thymus damage.

MSCs repair TECs and promote T-lymphocyte development

The proportion and number of TECs subpopulations were analyzed with flow cytometry on days 7 (supplemental Figure 3), 20, and 40 after HCT. Moreover, TECs expressing major histocompatibility complex class II (MHC II), a marker of TECs maturity, and autoimmune regulator (Aire) of mTECs (Aire-positive mTECs participate in the establishment of self-tolerance and regulatory T-cell [Treg] induction) were also evaluated.

Results revealed that the number of both cortical TECs and mTECs and the proportion of mTECs in TECs were significantly increased in MSC-GVHD mice compared with that in non–MSC-GVHD mice on day 40 (Figure 3A-B). Moreover, MSC-GVHD mice gained markedly enhanced MHC II expression on TECs when compared with non–MSC-GVHD mice (Figure 3C). Aire-positive mTECs were also detected to be increased in MSC-GVHD mice when compared with non–MSC-GVHD mice (Figure 3D).

These results suggest that MSCs promote the quantity and maturity of TECs. More importantly, MSCs may enhance the establishment of self-tolerance in the thymus by elevating Aire expression on mTECs.

Figure 4. MSCs promote intrathymic T-lymphocyte development. The number and proportion of $CD4^+CD8^+$ DP thymocytes and thymic Tregs, the ratio of $CD3^+CD4^+$:$CD3^+CD8^+$ T cells, Treg proportion, yield of $CD4^+$ T cells and Tregs in the blood were assessed on day 20 and day 40 after HCT with flow cytometry. The results are shown as mean ± SE (n = 4-6). (A) Representative flow patterns of $CD4^+CD8^+$ DP thymocytes. (B) Percentage and yield of DP thymocytes, data shown as the mean ± SE (n = 4-6). (C) Representative flow patterns of gated $CD4^+$ single-positive thymocytes shown as CD25 vs FoxP3. (D) Percentage and yield of $CD4^+CD25^+FoxP3^+$, data shown as the mean ± SE (n = 4-6). (E) Representative flow patterns of gated $CD3^+$ T cells in the blood shown as CD4 vs CD8. (F) The ratio of $CD4^+$ T cells to $CD8^+$ T cells and yield of $CD4^+$ T cells, data shown as the mean ± SE (n = 4-6). (G) Representative flow patterns of gated $CD4^+$ T cells in the peripheral blood shown as CD25 vs FoxP3. (H) Percentage and yield of $CD25^+FoxP3^+$ in $CD4^+$ T cells, data shown as the mean ± SE (n = 4-6). *P < .05; **P < .01; ***P < .001; ****P < .0001.

Downloaded from http://ashpublications.net/bloodadvances/article-pdf/7/18/5359/2079881/blooda_adv-2022-009646-main.pdf by guest on 12 June 2024

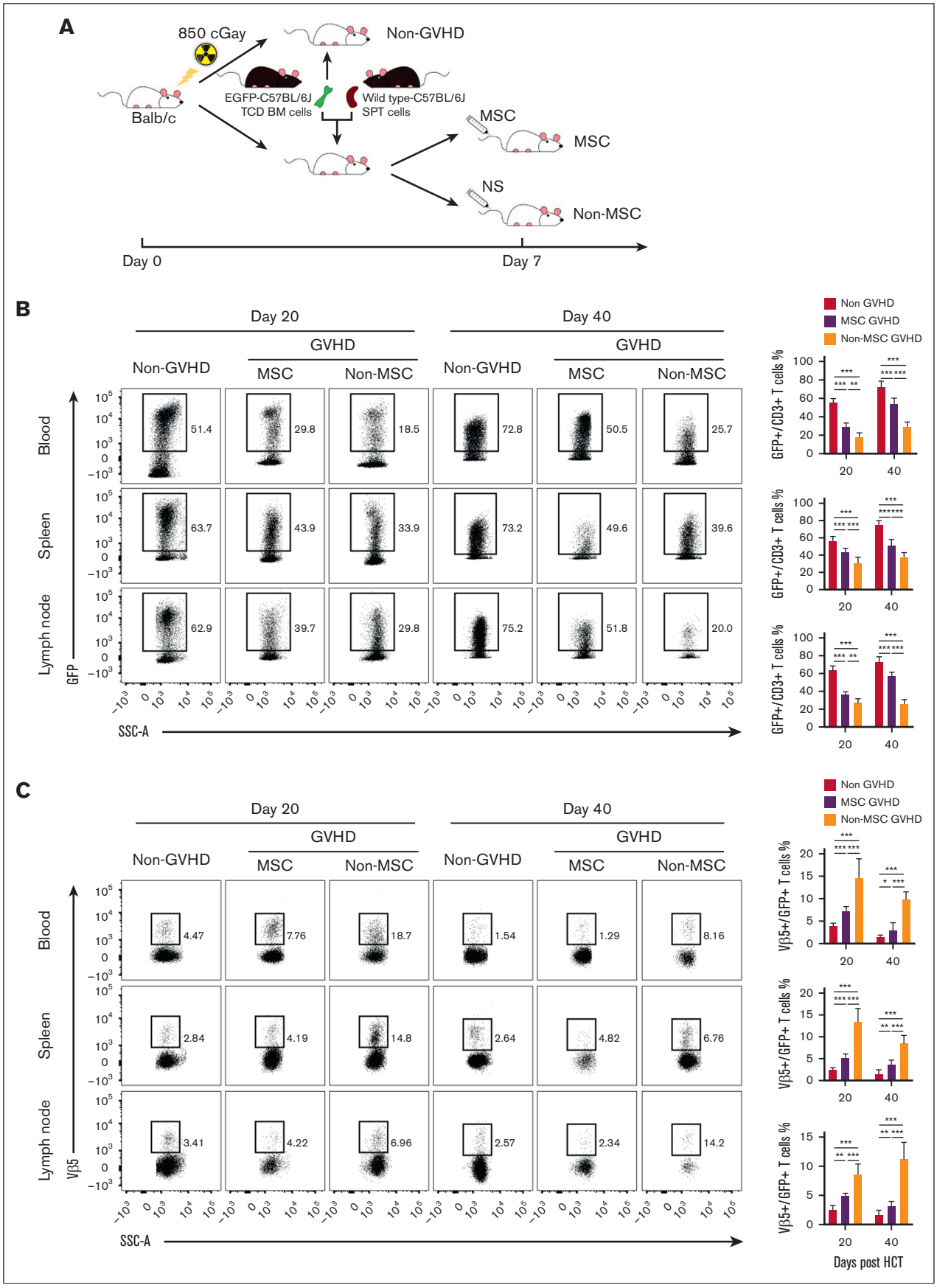

Figure 5.

Downloaded from http://ashpublications.net/bloodadvances/article-pdf/7/18/5359/2079881/blooda_adv-2022-009646-main.pdf by guest on 12 June 2024

To explore the effect of MSCs in intrathymic T-lymphocyte development, the yield of $CD4^+CD8^+$ double-positive (DP) thymocytes and thymic Tregs were analyzed in mice 7 (supplemental Figure 3), 20, and 40 days after HCT. Furthermore, the ratio of $CD3^+CD4^+$ T cells to $CD3^+CD8^+$ T cells, Treg proportion, yields of $CD4^+$ T cells and Tregs in the blood were also analyzed.

Results revealed that the number and proportion of DP thymocytes in the MSC-GVHD mice were significantly higher than in non–MSC-GVHD mice 20 and 40 days (Figure 4A-B) after HCT. The number and proportion of thymic Tregs were also markedly increased in MSC-GVHD mice 20 and 40 days after HCT compared with that in non–MSC-GVHD mice (Figure 4C-D).

The number of $CD4^+$ T cells and the ratio of $CD3^+CD4^+$ T cells to $CD3^+CD8^+$ T cells in the blood was significantly higher in MSC-GVHD mice than in non–MSC-GVHD mice 40 days after HCT (Figure 4E-F). The number and proportion of Tregs in the blood of the MSC-GVHD mice was also significantly higher than in non–MSC-GVHD mice 20 and 40 days after HCT (Figure 4G-H).

To further verify whether MSCs can promote de novo generation of T cells, mice were injected with TCD-BM from EGFP-transgenic C57BL/6J and splenocytes from wild-type C57BL/6 donors (Figure 5A). Using flow cytometry, GFP expression can be detected in the majority of thymus-dependent de novo T cells, whereas it can not be detected in T cells expanded through thymus-independent pathway. Results showed that on day 20 after HCT, the proportion of GFP^+ T cells in the peripheral blood, spleen, and lymph nodes of the non-GVHD group accounted for >50% of $CD3^+$ T cells, whereas the peripheral T cells in the GVHD groups were mainly derived from donor T cells in graft. Compared with the non-MSC group, the proportion of GFP^+ T cells in the MSC-GVHD group was significantly higher (Figure 5B). Similarly, on day 40 after HCT, GFP^+ T cells in the non-GVHD group were predominant in the peripheral T cells pool and further increased in GVHD groups. The proportion of GFP^+ T cells in the MSC-GVHD mice was still higher than that in non–MSC-GVHD mice (Figure 5B), which suggested that MSCs promoted de novo generation of T cells.

Mouse mammary tumor virus (MMTV)-encoded superantigens can influence the murine T-cell repertoire, and the T-cell response to MMTV superantigens is restricted by T-cell receptor Vβ chains, such as $CD4^+CD8^+$ thymocytes expressing the Vβ5 chains that undergo programmed cell death in BALB/c mice carrying exogenous MMTV-8.[37-39] Therefore, detecting the proportion of $V\beta5^+$ T cells in thymus-dependent de novo T cells via flow cytometry can reflect the negative selection of recipient thymus. Results showed that the proportion of $V\beta5^+$ in GFP^+ T cells in the peripheral blood, spleen, and lymph nodes of the GVHD mice was significantly higher compared with that in the non-GVHD mice on day 20 after HCT, whereas the intervention of MSCs significantly reduced the proportion of $V\beta5^+$ in GFP^+ T cells compared with that in the non-MSC group. Similarly, the same results were observed on day 40 after HCT (Figure 5C), which suggest that MSCs improved the negative selection of GVHD mice.

These results suggest that MSCs promote the de novo generation of T cells and self-tolerance establishment, which may be the underlying mechanism of MSCs reduction of incidence and severity of cGVHD in aGVHD mice.

$CCR9^+$ MSCs are the major effector cells ameliorating cGVHD

To explore the mechanism of MSCs homing to the thymus, chemokine expression of the thymus in severe-GVHD mice 7 days after HCT and chemokine receptors of MSCs were analyzed. CCL25 was found to be the most expressed chemokine in the thymus of GVHD mice (Figure 6A), whereas CCR9, the only specific receptor for CCL25, was detected in MSCs (Figure 6B-C). To further determine whether the CCL25-CCR9 axis guides MSCs to home to the thymus, CCR9-overexpressed MSCs ($MSCs^{CCR9+}$) and CCR9-knockdown MSCs ($MSCs^{CCR9-}$) were prepared (Figure 6B-C), and their thymic homing ability compared with that of $MSCs^{CCR9WT}$ on days 1, 7, and 14 after MSCs infusion. The results showed that $MSCs^{CCR9WT}$ was distributed mainly in the cortex of the thymus, with a small amount in the medulla, 7 days after MSCs infusion. $MSCs^{CCR9-}$ were almost undetectable in the medulla and appeared sporadically in the cortex. A significantly large number of $MSCs^{CCR9+}$ were present in the thymus, especially in the medulla when compared with $MSCs^{CCR9WT}$ and $MSCs^{CCR9-}$ (Figure 6D). The distribution of MSCs in the thymus on days 1 (supplemental Figure 4A) and 14 (supplemental Figure 4B) after infusion were similar to that on day 7.

To determine whether $CCR9^+$ MSCs were the major effector cells to ameliorate cGVHD, we assessed the cutaneous cGVHD score and survival rate 60 days after HCT in the 3 groups. The results showed that MSC^{CCR9+} GVHD mice displayed lower cutaneous cGVHD scores than MSC^{CCR9WT} GVHD and MSC^{CCR9-} GVHD mice (Figure 6E-F). Moreover, ~90% of MSC^{CCR9+} GVHD mice survived for >60 days after HCT, compared with ~75% of MSC^{CCR9WT} GVHD mice and ~ 50% of MSC^{CCR9-} GVHD mice (Figure 6G).

These data indicate that MSCs depend on the CCL25-CCR9 axis for homing to the thymus and that $CCR9^+$ MSCs are the major effector cells repairing the thymus and ameliorating cGVHD.

Figure 5. MSCs promote de novo generation and negative selection of T cells. Approximately 2.5×10^6 TCD-BM from EGFP-transgenic C57BL/6J donor alone (non-GVHD) or these plus 1×10^6 splenocytes from WT C57BL/6J donor were transplanted into BALB/c mice. Recipients treated with WT MSCs (MSC-GVHD) or normal saline (non–MSC-GVHD) on day 7 after HCT. (A) Schematic diagram depicting generation of the EGFP-BM GVHD murine model. (B) Representative fluorescence-activated cell sorting (FACS) plots (left) and quantification (right) of GFP^+ T cells in $CD3^+$ T cells of the blood, spleen, and lymph node of recipients on day 20 and day 40 after transplantation (n = 6 mice for each group). (C) Representative FACS plots (left) and quantification (right) of $GFP^+V\beta5^+$ T cells in $CD3^+$ T cells of the blood, spleen, and lymph node of recipients on day 20 and day 40 after transplantation (n = 6 mice for each group). $^*P < .05$; $^{**}P < .01$; $^{***}P < .001$.

Downloaded from http://ashpublications.net/bloodadvances/article-pdf/7/18/5359/2079881/blooda_adv-2022-009646-main.pdf by guest on 12 June 2024

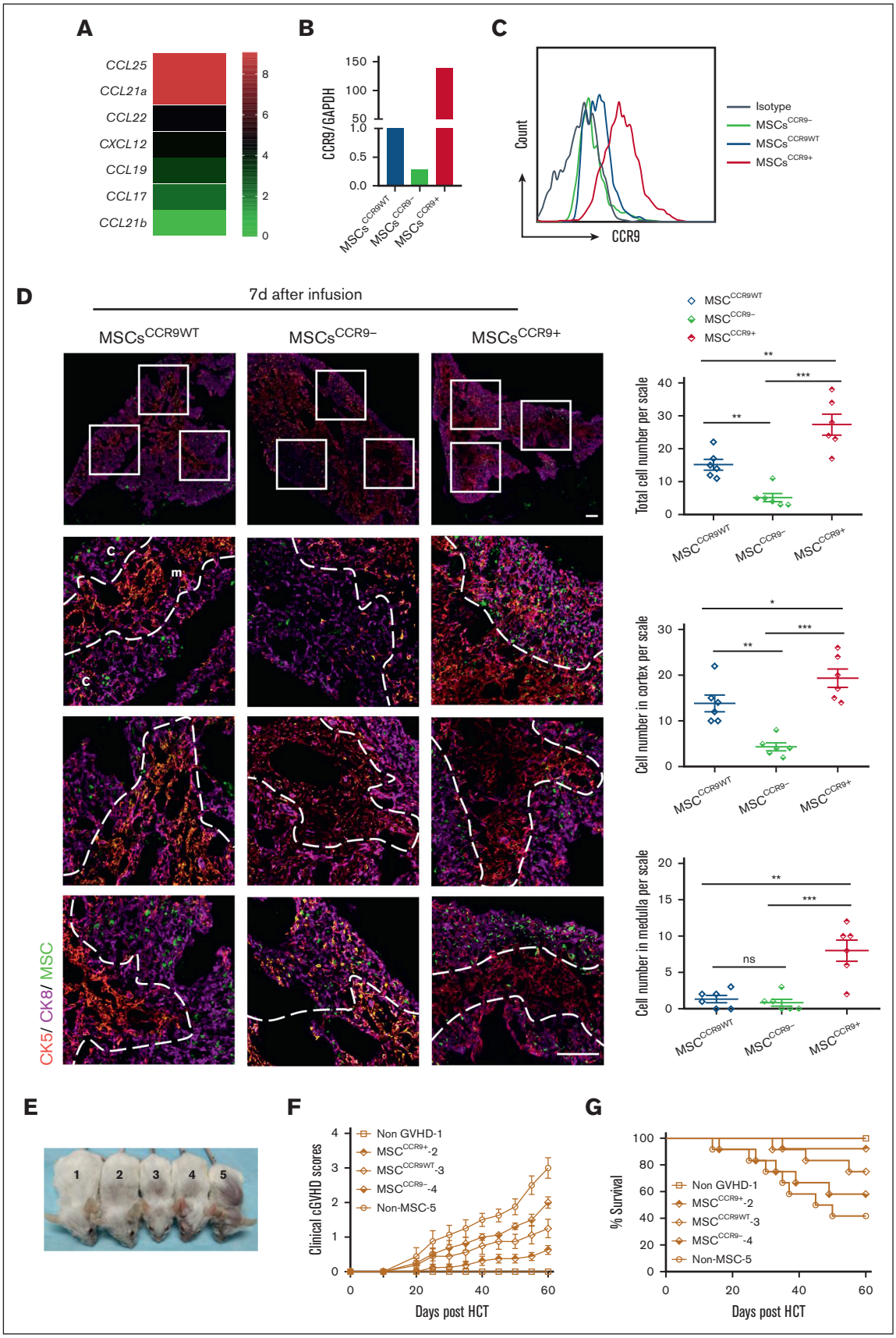

Figure 6.

Downloaded from http://ashpublications.net/bloodadvances/article-pdf/7/18/5359/2079881/blooda_adv-2022-009646-main.pdf by guest on 12 June 2024

Discussion

Thymus damage caused by aGVHD results in limited thymus-dependent T-cell reconstitution, negative selection failure, and Treg loss, which contributes to cGVHD.[5,7-9,11] Therefore, strategies that prevent or treat cGVHD may be efficacious if they alleviate thymus damage caused by aGVHD.[11] Previous preclinical studies exploiting castration, thymic transplantation, adoptive cell therapies, hormones/growth factors, and cytokines have demonstrated enhanced thymic function and immune reconstitution after allo-HSCT.[40-42] However, current agents are failing, in terms of safety and efficacy, in clinical settings.[40,43] This study confirmed that aGVHD resulted in thymus damage and that the incidence and severity of cGVHD were related to the degree of thymus damage in a murine GVHD model. The disruption of thymic architecture recovered, and the incidence and severity of subsequent cGVHD decreased after MSCs treatment. These findings suggest that MSCs may be effective candidates for thymus repair and GVHD treatment.

T-cell development depends on the thymus microenvironment.[44,45] The thymic microenvironment consists of a complex mixture of epithelial and mesenchymal cells, interdigitating dendritic cells, and macrophages.[44] Cortical TECs in the cortex trigger positive selection to generate $CD4^+CD8^+$ DP T cells, whereas mTECs together with dendritic cells enriched at the cortical-medullary junction and the medulla are responsible for negative selection to generate self-tolerance.[46] Aire in mTECs drives organ-specific antigen expression and mediates the negative selection of autoreactive T cells as well as the generation of Tregs.[47,48] MSCs, as a subset of stromal stem cells in the thymus microenvironment, play an important role in thymic development and regeneration.[49,50] To date, the mechanism by which MSCs protect or repair TECs has not been clearly explained. Some studies found that MSCs play a crucial role in TECs proliferation by secreting KGF, IGF1, IGF2, FGF7, BMP4, and retinoic acid.[51-57] Liu et al demonstrated that MSCs could facilitate the functional maturation of residual thymic epithelial precursors in the $Foxn1^{-/-}$ thymus.[50] In this study, MSCs were found to repair the thymus as shown by promoting the quantity and maturity of TECs and elevating the proportion of $Aire^+$ mTECs in GVHD mice. Based on relevant literature, we speculated that MSCs might promote the proliferation and maturity of TECs, or protect TECs from further destruction through direct cell-to-cell contact and indirectly secreted cytokines, thus improving the positive and negative selection of thymocytes, as well as the recovery of immune balance in the peripheral.

The therapeutic efficacy of MSCs largely relies upon their ability to home to target tissues.[25,26] Chemokines and their receptors are major mediators for MSCs homing to target tissues.[29,32] In this study, CCL25, also known as thymus-expressed chemokine, was detected to be highly expressed in the thymus of GVHD mice. By comparing the thymus homing and GVHD amelioration properties of $MSCs^{CCR9WT}$, $MSCs^{CCR9+}$, and $MSCs^{CCR9-}$, we found that $CCR9^+$ MSCs are the major effector cells that repair the thymus and ameliorate GVHD. Furthermore, $MSCs^{CCR9-}$ were also detected in the thymus, indicating that there might be another axis guiding MSCs homing to the thymus.

In summary, this study demonstrates that MSCs can decrease the severity of cGVHD in a murine GVHD model. The underlying mechanism is that MSCs repair the damaged thymus caused by aGVHD. Unlike previous studies on the immunomodulation of MSCs that focused on their impact on the peripheral immune pool, our study provides a new viewpoint of MSCs ameliorating GVHD and other autoimmune diseases.

Acknowledgments

This work was supported by the Major Program of National Natural Science Foundation of China (82293634), the National Natural Science Foundation of China (81970161 and 82170215), Jiangsu Natural Science Foundation (BK20210086), and National Key Research and Development Program of China (2022YFA1105003, 2017YFA0105500, and 2017YFA105504).

Authorship

Contribution: X.Z. performed the majority of the experiments, analyzed and interpreted related data, and helped write the manuscript; K.Z. and L.X. helped with the experiments and development of the overall concept behind the study; J.H., S.L., S.C., R.L, J.X., and R.X. helped with the experiments and data interpretation; Y.Z. performed the lentiviral vector transduction; A.P.X. helped develop the concept behind the study and critically reviewed the manuscript; H.J. helped develop the concept behind the study, supervised the experiments, and wrote the manuscript; and Q.L. developed the overall concept behind the study, supervised the experiments, and wrote the manuscript.

Conflict-of-interest disclosure: The authors declare no competing financial interests.

Figure 6. $CCR9^+$ MSCs are the major effector cells homing to the thymus and ameliorating cGVHD in mice. (A) Thymus glands of severe-GVHD recipients were harvested 7 days after HCT for RNA isolation and RNA-sequencing microarray analysis. Heatmaps of RNA expression of *CCL25, CXCL2, CCL19, CCL21, CCL17*, and *CCL22* are shown as (mean + 1) centered $\log_2$ expression. CCR9-WT MSCs ($MSCs^{CCR9WT}$) from EGFP-transgenic mice were transduced with lentivirus to overexpress CCR9 ($MSCs^{CCR9+}$) and lentivirus encoded CCR9-specific short hairpin RNA ($MSCs^{CCR9-}$). Quantitative reverse transcription polymerase chain reaction (qRT-PCR) (B) and flow cytometry (C) were used to analyze the messenger RNA (mRNA) or protein expression of CCR9 in $MSCs^{CCR9WT}$, $MSCs^{CCR9+}$, and $MSCs^{CCR9-}$. EGFP-expressing $MSCs^{CCR9WT}$, $MSCs^{CCR9+}$, and $MSCs^{CCR9-}$ were intravenously infused into mice with severe-GVHD on day 7 after HCT. (D) The presence and distribution of EGFP-expressing MSCs were examined via in situ immunofluorescence staining on day 7 after infusion. Total number and distribution of $EGFP^+$ cells in the cortex and medulla were quantified per microscopic scale of thymus cryosections in triplicate mice, dotted lines trace the border between the cortex and medulla. Data are presented as mean ± SE. Signals: EGFP, (green, MSCs); CK8 (purple, highly expressed in the cortex and lowly expressed in the medulla); CK5, (red, expressed in the medulla). Scale bars, 50 μm. (E) Mice from each group on day 60 after HCT (1, non-GVHD; 2, MSC^{CCR9+} GVHD; 3, MSC^{CCR9WT} GVHD; 4, MSC^{CCR9-} GVHD; and 5, non–MSC GVHD). (F) Cutaneous cGVHD symptom score (MSC^{CCR9WT} vs MSC^{CCR9+}, $P < .01$; MSC^{CCR9+} vs MSC^{CCR9-}, $P < .001$; MSC^{CCR9WT} vs MSC^{CCR9-}, ns). (G) Survival curve (MSC^{CCR9+} vs MSC^{CCR9-}, $P < .05$). *$P < .05$; **$P < .01$; ***$P < .001$.

Downloaded from http://ashpublications.net/bloodadvances/article-pdf/7/18/5359/2079881/blooda_adv-2022-009646-main.pdf by guest on 12 June 2024

ORCID profiles: J.H., 0000-0003-3872-6301; R.X., 0000-0001-7269-4708; Y.Z., 0000-0002-5735-207X; Q.L., 0000-0003-4015-3952.

Correspondence: Qifa Liu, Department of Hematology, Nanfang Hospital, Southern Medical University, Guangzhou 510515, China; email: liuqifa628@163.com; Hua Jin, Department of Hematology, Nanfang Hospital, Southern Medical University, Guangzhou 510515, China; email: echohua1124@163.com; and Andy Peng Xiang, Center for Stem Cell Biology and Tissue Engineering, Sun Yat-Sen University, Guangzhou 510275, China; email: xiangp@mail.sysu.edu.cn.

References

1. Martin PJ, Counts GW Jr, Appelbaum FR, et al. Life expectancy in patients surviving more than 5 years after hematopoietic cell transplantation. *J Clin Oncol*. 2010;28(6):1011-1016.
2. Wingard JR, Majhail NS, Brazauskas R, et al. Long-term survival and late deaths after allogeneic hematopoietic cell transplantation. *J Clin Oncol*. 2011;29(16):2230-2239.
3. Arai S, Arora M, Wang T, et al. Increasing incidence of chronic graft-versus-host disease in allogeneic transplantation: a report from the Center for International Blood and Marrow Transplant Research. *Biol Blood Marrow Transplant*. 2015;21(2):266-274.
4. Socié G, Ritz J. Current issues in chronic graft-versus-host disease. *Blood*. 2014;124(3):374-384.
5. Hollander GA, Widmer B, Burakoff SJ. Loss of normal thymic repertoire selection and persistence of autoreactive T cells in graft vs host disease. *J Immunol*. 1994;152(4):1609-1617.
6. van den Brink MR, Moore E, Ferrara JL, Burakoff SJ. Graft-versus-host-disease-associated thymic damage results in the appearance of T cell clones with anti-host reactivity. *Transplantation*. 2000;69(3):446-449.
7. Krenger W, Blazar BR, Hollander GA. Thymic T-cell development in allogeneic stem cell transplantation. *Blood*. 2011;117(25):6768-6776.
8. Wu T, Young JS, Johnston H, et al. Thymic damage, impaired negative selection, and development of chronic graft-versus-host disease caused by donor CD4+ and CD8+ T cells. *J Immunol*. 2013;191(1):488-499.
9. Dertschnig S, Hauri-Hohl MM, Vollmer M, Hollander GA, Krenger W. Impaired thymic expression of tissue-restricted antigens licenses the de novo generation of autoreactive CD4+ T cells in acute GVHD. *Blood*. 2015;125(17):2720-2723.
10. Jin H, Ni X, Deng R, et al. Antibodies from donor B cells perpetuate cutaneous chronic graft-versus-host disease in mice. *Blood*. 2016;127(18):2249-2260.
11. MacDonald KP A, Hill GR, Blazar BR. Chronic graft-versus-host disease: biological insights from preclinical and clinical studies. *Blood*. 2017;129(1):13-21.
12. Anderson G, Takahama Y. Thymic epithelial cells: working class heroes for T cell development and repertoire selection. *Trends Immunol*. 2012;33(6):256-263.
13. Han J, Zuniga-Pflucker JCA. 2020 view of thymus stromal cells in T cell development. *J Immunol*. 2021;206(2):249-256.
14. Patenaude J, Perreault C. Thymic mesenchymal cells have a distinct transcriptomic profile. *J Immunol*. 2016;196(11):4760-4770.
15. Baiguera S, Jungebluth P, Mazzanti B, Macchiarini P. Mesenchymal stromal cells for tissue-engineered tissue and organ replacements. *Transpl Int*. 2012;25(4):369-382.
16. Uccelli A, Moretta L, Pistoia V. Mesenchymal stem cells in health and disease. *Nat Rev Immunol*. 2008;8(9):726-736.
17. Zhao S, Wehner R, Bornhäuser M, Wassmuth R, Bachmann M, Schmitz M. Immunomodulatory properties of mesenchymal stromal cells and their therapeutic consequences for immune-mediated disorders. *Stem Cells Dev*. 2010;19(5):607-614.
18. Fisher SA, Cutler A, Doree C, et al. Mesenchymal stromal cells as treatment or prophylaxis for acute or chronic graft-versus-host disease in haematopoietic stem cell transplant (HSCT) recipients with a haematological condition. *Cochrane Database Syst Rev*. 2019;1:CD009768.
19. Gao L, Zhang Y, Hu B, et al. Phase II multicenter, randomized, double-blind controlled study of efficacy and safety of umbilical cord–derived mesenchymal stromal cells in the prophylaxis of chronic graft-versus-host disease after HLA-haploidentical stem-cell transplantation. *J Clin Oncol*. 2016;34(24):2843-2850.
20. Zhao K, Lin R, Fan Z, et al. Mesenchymal stromal cells plus basiliximab, calcineurin inhibitor as treatment of steroid-resistant acute graft-versus-host disease: a multicenter, randomized, phase 3, open-label trial. *J Hematol Oncol*. 2022;15(1):22.
21. Zhao K, Lou R, Huang F, et al. Immunomodulation effects of mesenchymal stromal cells on acute graft-versus-host disease after hematopoietic stem cell transplantation. *Biol Blood Marrow Transplant*. 2015;21(1):97-104.
22. Zhao K, Zhang X, Liu Q. Bone marrow-derived mesenchymal stromal cells promote thymopoiesis and function recovery in acute graft-versus-host disease murine models. *Blood*. 2017;130(suppl 1):5444.
23. Hu K, Wang Mh, Fan C, Wang L, Guo M, Ai Hs. CM-DiI labeled mesenchymal stem cells homed to thymus inducing immune recovery of mice after haploidentical bone marrow transplantation. *Int Immunopharmacol*. 2011;11(9):1265-1270.
24. Zhan Y, Wang L, Liu G, et al. The reparative effects of human adipose-derived mesenchymal stem cells in the chemotherapy-damaged thymus. *Stem Cells Dev*. 2019;28(3):186-195.

Downloaded from http://ashpublications.net/bloodadvances/article-pdf/7/18/5359/2079881/blooda_adv-2022-009646-main.pdf by guest on 12 June 2024

25. Li H, Jiang Y, Jiang X, et al. CCR7 guides migration of mesenchymal stem cell to secondary lymphoid organs: a novel approach to separate GvHD from GvL effect. *Stem Cells*. 2014;32(7):1890-1903.
26. Zhang X, Huang W, Chen X, et al. CXCR5-overexpressing mesenchymal stromal cells exhibit enhanced homing and can decrease contact hypersensitivity. *Mol Ther*. 2017;25(6):1434-1447.
27. Vicari AP, Figueroa DJ, Hedrick JA, et al. TECK: a novel CC chemokine specifically expressed by thymic dendritic cells and potentially involved in T cell development. *Immunity*. 1997;7(2):291-301.
28. Wurbel MA, Philippe JM, Nguyen C, et al. The chemokine TECK is expressed by thymic and intestinal epithelial cells and attracts double- and single-positive thymocytes expressing the TECK receptor CCR9. *Eur J Immunol*. 2000;30(1):262-271.
29. Cornelissen AS, Maijenburg MW, Nolte MA, Voermans C. Organ-specific migration of mesenchymal stromal cells: who, when, where and why? *Immunol Lett*. 2015;168(2):159-169.
30. Binger T, Stich S, Andreas K, et al. Migration potential and gene expression profile of human mesenchymal stem cells induced by CCL25. *Exp Cell Res*. 2009;315(8):1468-1479.
31. Ullah M, Eucker J, Sittinger M, Ringe J. Mesenchymal stem cells and their chondrogenic differentiated and dedifferentiated progeny express chemokine receptor CCR9 and chemotactically migrate toward CCL25 or serum. *Stem Cell Res Ther*. 2013;4(4):1-16.
32. Andreas K, Sittinger M, Ringe J. Toward in situ tissue engineering: chemokine-guided stem cell recruitment. *Trends Biotechnol*. 2014;32(9):483-492.
33. Spinnen J, Ringe J, Sittinger M. CCL25 chemokine-guided stem cell attraction: an assessment of possible benefits and risks. *Regen Med*. 2018;13(7):833-844.
34. Zhu H, Guo ZK, Jiang XX, et al. A protocol for isolation and culture of mesenchymal stem cells from mouse compact bone. *Nat Protoc*. 2010;5(3):550-560.
35. Lockridge JL, Zhou Y, Becker YA, et al. Mice engrafted with human fetal thymic tissue and hematopoietic stem cells develop pathology resembling chronic graft-versus-host disease. *Biol Blood Marrow Transplant*. 2013;19(9):1310-1322.
36. Deng R, Hurtz C, Song Q, et al. Extrafollicular CD4(+) T-B interactions are sufficient for inducing autoimmune-like chronic graft-versus-host disease. *Nat Commun*. 2017;8(1):978.
37. Labrecque N, McGrath H, Subramanyam M, Huber BT, Sekaly RP. Human T cells respond to mouse mammary tumor virus-encoded superantigen: V beta restriction and conserved evolutionary features. *J Exp Med*. 1993;177(6):1735-1743.
38. Acha-Orbea H, MacDonald HR. Superantigens of mouse mammary tumor virus. *Annu Rev Immunol*. 1995;13(1):459-486.
39. Simpson E. T cell repertoire selection by mouse mammary tumour viruses. *Eur J Immunogenet*. 1993;20(2):137-149.
40. Velardi E, Dudakov JA, van den Brink MR. Clinical strategies to enhance thymic recovery after allogeneic hematopoietic stem cell transplantation. *Immunol Lett*. 2013;155(1-2):31-35.
41. El-Kadiry AE, Rafei M. Restoring thymic function: then and now. *Cytokine*. 2019;120:202-209.
42. Dertschnig S, Nusspaumer G, Ivanek R, Hauri-Hohl MM, Holländer GA, Krenger W. Epithelial cytoprotection sustains ectopic expression of tissue-restricted antigens in the thymus during murine acute GVHD. *Blood*. 2013;122(5):837-841.
43. Goldberg JD, Zheng J, Castro-Malaspina H, et al. Palifermin is efficacious in recipients of TBI-based but not chemotherapy-based allogeneic hematopoietic stem cell transplants. *Bone Marrow Transplant*. 2013;48(1):99-104.
44. Anderson G, Lane PJL, Jenkinson EJ. Generating intrathymic microenvironments to establish T-cell tolerance. *Nat Rev Immunol*. 2007;7(12):954-963.
45. Rodewald HR. Thymus organogenesis. *Annu Rev Immunol*. 2008;26:355-388.
46. Bleul CC, Corbeaux T, Reuter A, Fisch P, Mönting JS, Boehm T. Formation of a functional thymus initiated by a postnatal epithelial progenitor cell. *Nature*. 2006;441(7096):992-996.
47. Aschenbrenner K, D'Cruz LM, Vollmann EH, et al. Selection of Foxp3+ regulatory T cells specific for self antigen expressed and presented by Aire+ medullary thymic epithelial cells. *Nat Immunol*. 2007;8(4):351-358.
48. Perniola R. Twenty years of AIRE. *Front Immunol*. 2018;9:98.
49. Itoi M, Tsukamoto N, Yoshida H, Amagai T. Mesenchymal cells are required for functional development of thymic epithelial cells. *Int Immunol*. 2007;19(8):953-964.
50. Liu G, Wang L, Pang T, et al. Umbilical cord-derived mesenchymal stem cells regulate thymic epithelial cell development and function in Foxn1(-/-) mice. *Cell Mol Immunol*. 2014;11(3):275-284.
51. Erickson M, Morkowski S, Lehar S, et al. Regulation of thymic epithelium by keratinocyte growth factor. *Blood*. 2002;100(9):3269-3278.
52. Balciunaite G, Keller MP, Balciunaite E, et al. Wnt glycoproteins regulate the expression of FoxN1, the gene defective in nude mice. *Nat Immunol*. 2002;3(11):1102-1108.
53. Bleul CC, Boehm T. BMP signaling is required for normal thymus development. *J Immunol*. 2005;175(8):5213-5221.
54. Chu YW, Schmitz S, Choudhury B, et al. Exogenous insulin-like growth factor 1 enhances thymopoiesis predominantly through thymic epithelial cell expansion. *Blood*. 2008;112(7):2836-2846.
55. Gordon J, Patel SR, Mishina Y, Manley NR. Evidence for an early role for BMP4 signaling in thymus and parathyroid morphogenesis. *Dev Biol*. 2010;339(1):141-154.

Downloaded from http://ashpublications.net/bloodadvances/article-pdf/7/18/5359/2079881/blooda_adv-2022-009646-main.pdf by guest on 12 June 2024

56. Kvell K, Fejes AV, Parnell SM, Pongracz JE. Active Wnt/beta-catenin signaling is required for embryonic thymic epithelial development and functionality ex vivo. *Immunobiology*. 2014;219(8):644-652.

57. Sitnik KM, Kotarsky K, White AJ, Jenkinson WE, Anderson G, Agace WW. Mesenchymal cells regulate retinoic acid receptor-dependent cortical thymic epithelial cell homeostasis. *J Immunol*. 2012;188(10):4801-4809.

Downloaded from http://ashpublications.net/bloodadvances/article-pdf/7/18/5359/2079881/blooda_adv-2022-009646-main.pdf by guest on 12 June 2024